

Late-time Chandra Observations of GRB X-ray Afterglows and a Numerical Simulation-based Jet Model

Binbin Zhang

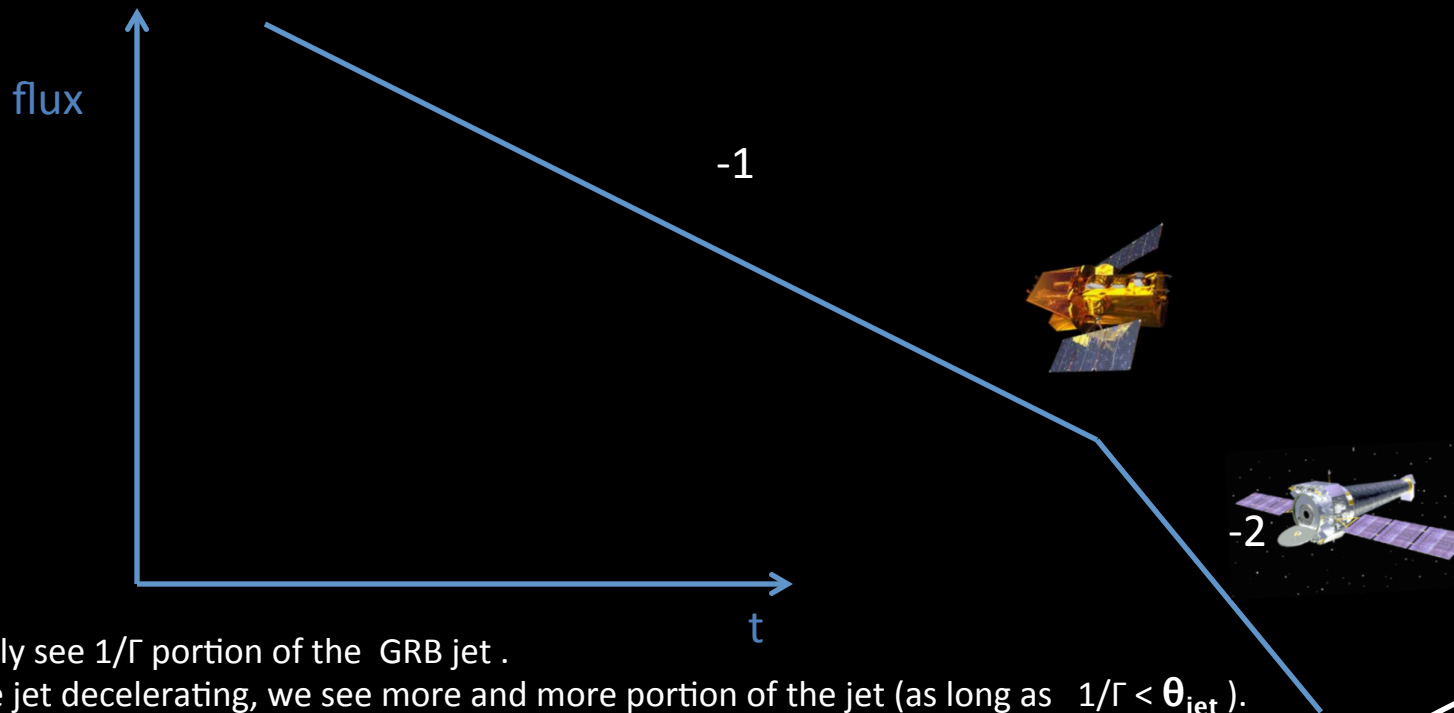


Collaborators

- David N. Burrows (PSU)
- Hendrik van Eerten (NYU)
- Andrew MacFadyen (NYU)
- Geoffrey Scott Ryan (NYU)
- Judith Racusin (GSFC)
- Eleonora Troja (GSFC)

Chandra observes **later** and **deeper**

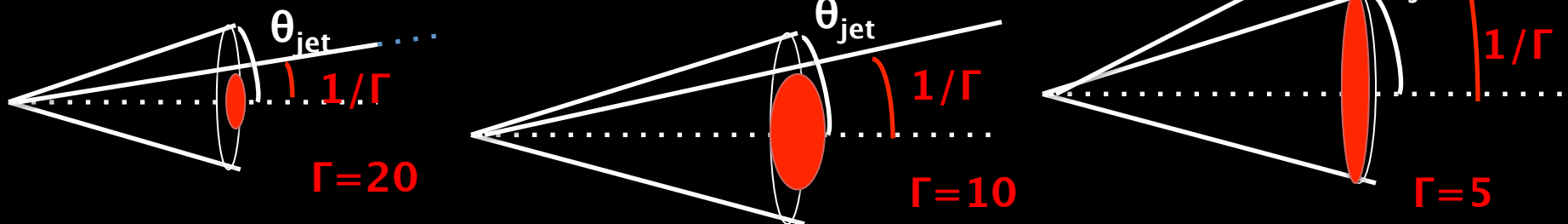
- more capable to detect jet-breaks in GRB afterglows



We only see $1/\Gamma$ portion of the GRB jet .

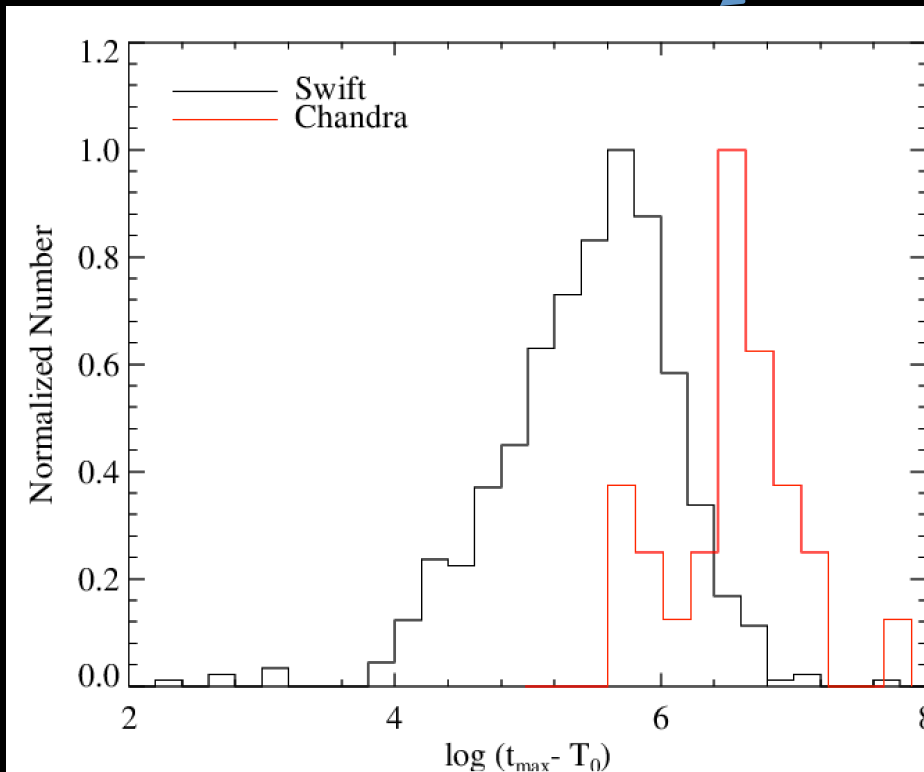
As the jet decelerating, we see more and more portion of the jet (as long as $1/\Gamma < \theta_{\text{jet}}$).

A jet-break occurs when the relativistic GRB jet decelerate to $1/\Gamma > \theta_{\text{jet}}$

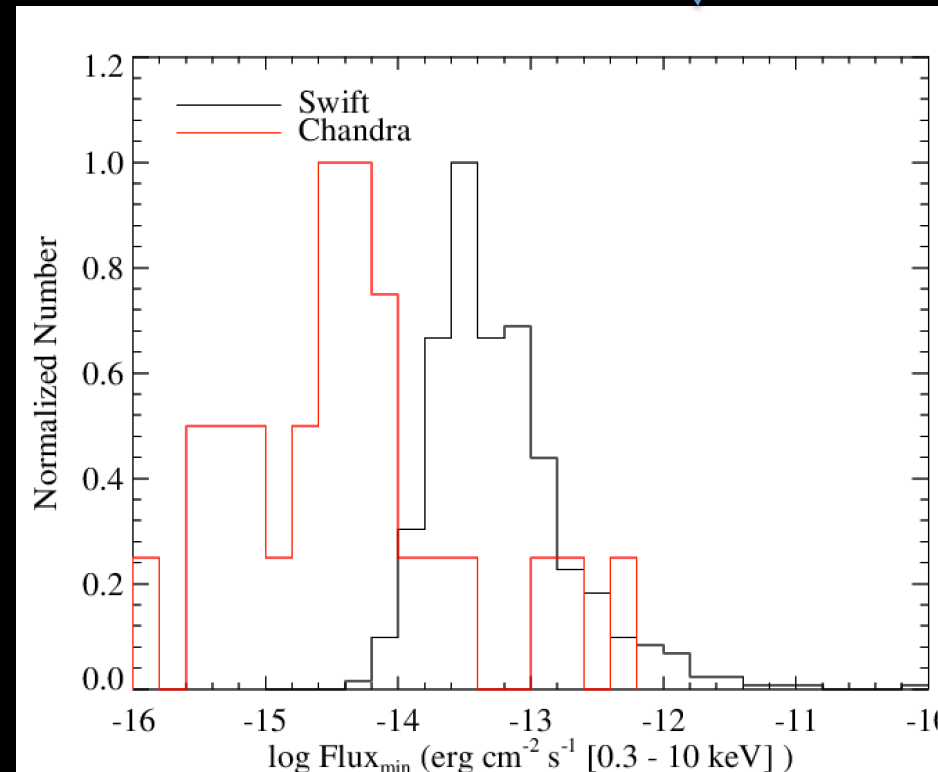


Chandra observes **later** and **deeper**

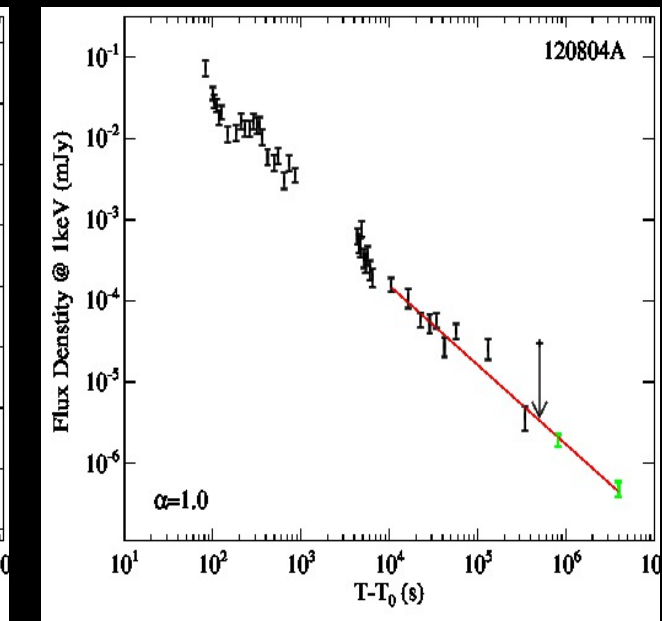
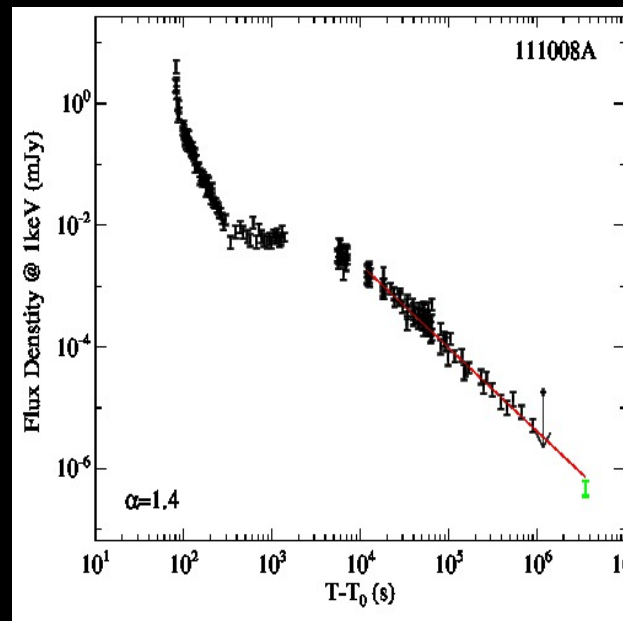
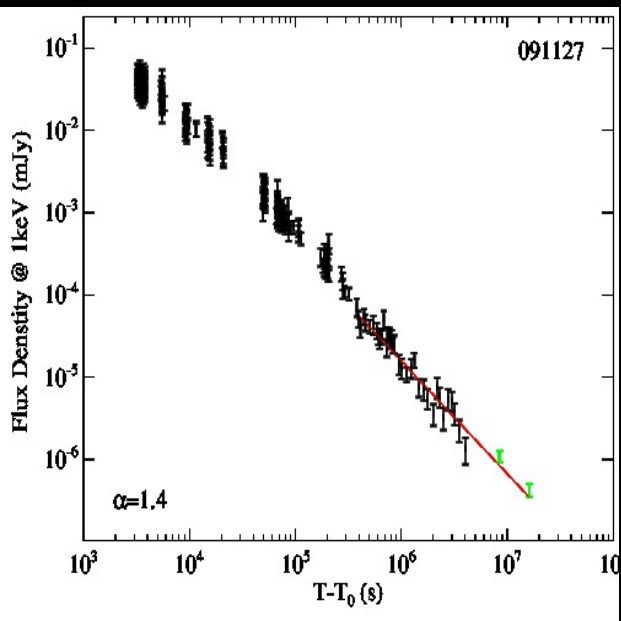
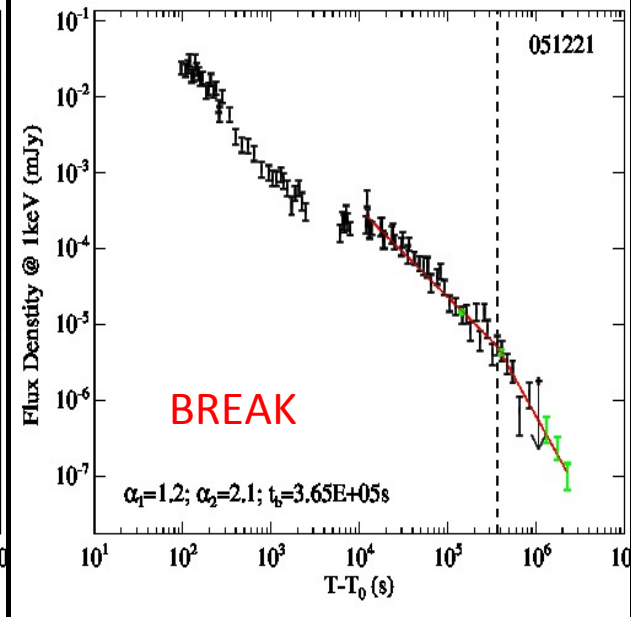
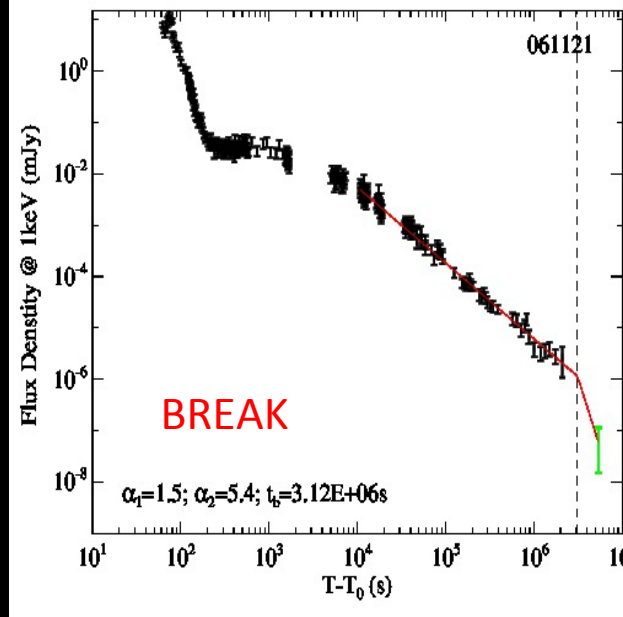
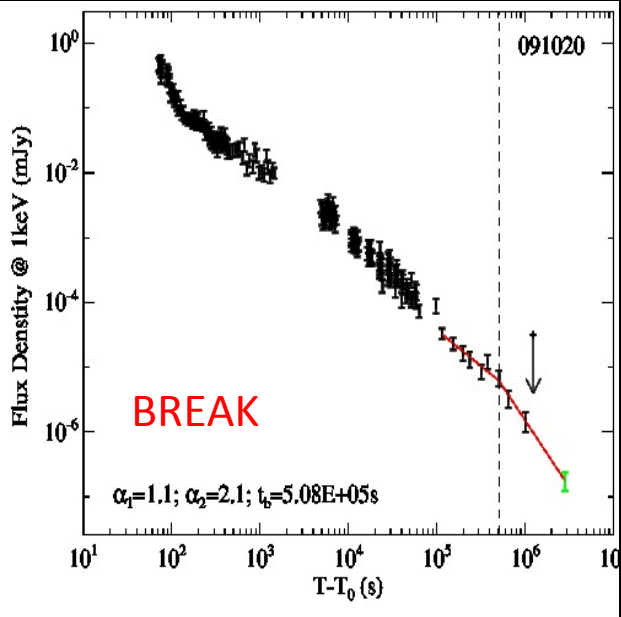
a sample of **27** GRBs with late-time Chandra observations



Follow-up time



Follow-up flux

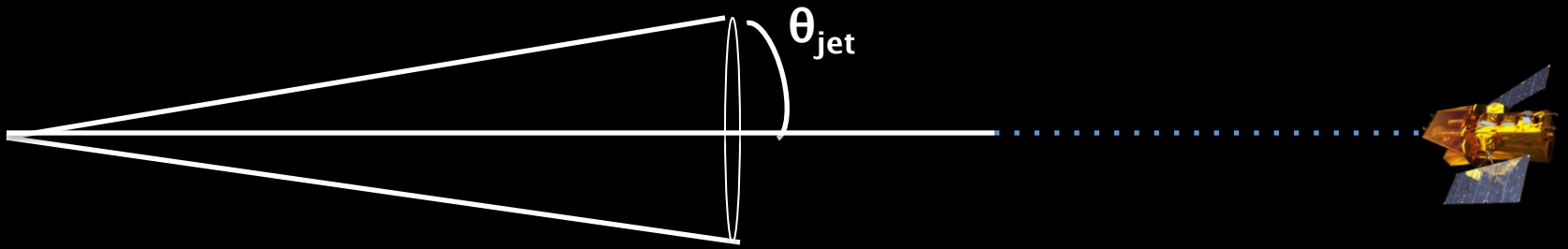


What are in the Chandra GRB Zoo?

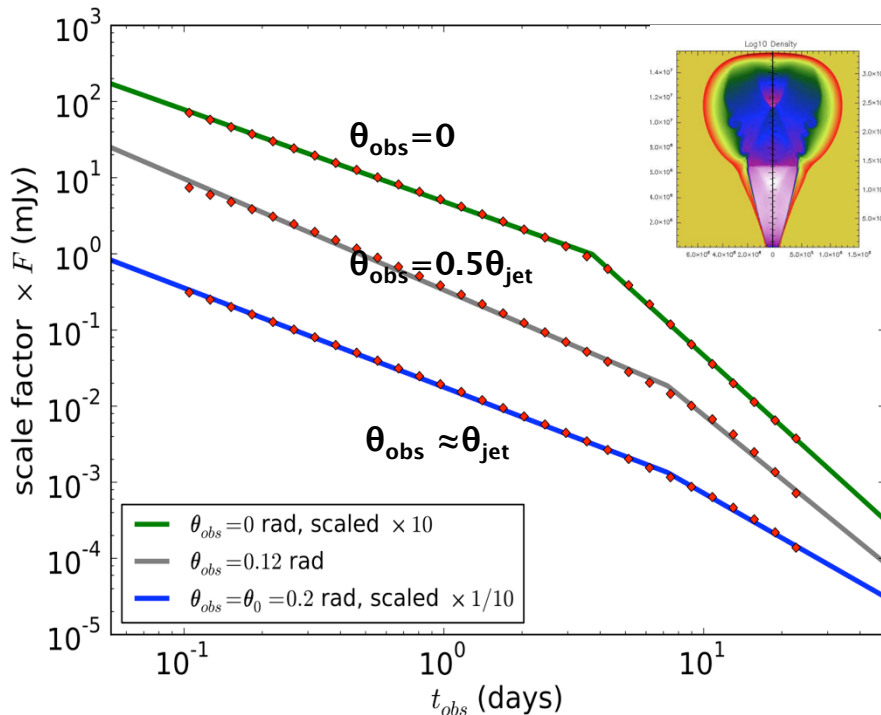
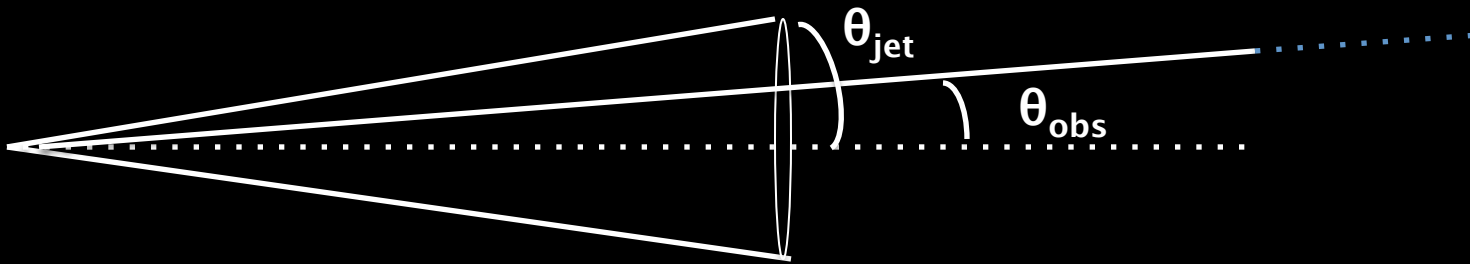
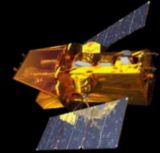
- Jet-Breaks :
 - shown in 50% of the whole sample (13/27)
 - For comparison, jet-breaks shown in 12% of Swift sample (e.g, Liang et al. 2008, Racusin et al. 2009)
- Later Jet-breaks
 - Chandra jet-breaks occur much later (10 times later) than Swift jet-breaks
- Non-Breaks :
 - Some bursts show no sign for break up to 1.6×10^7 s

Does No Jet-break mean No Jet?

Why do some jet-breaks are hidden?



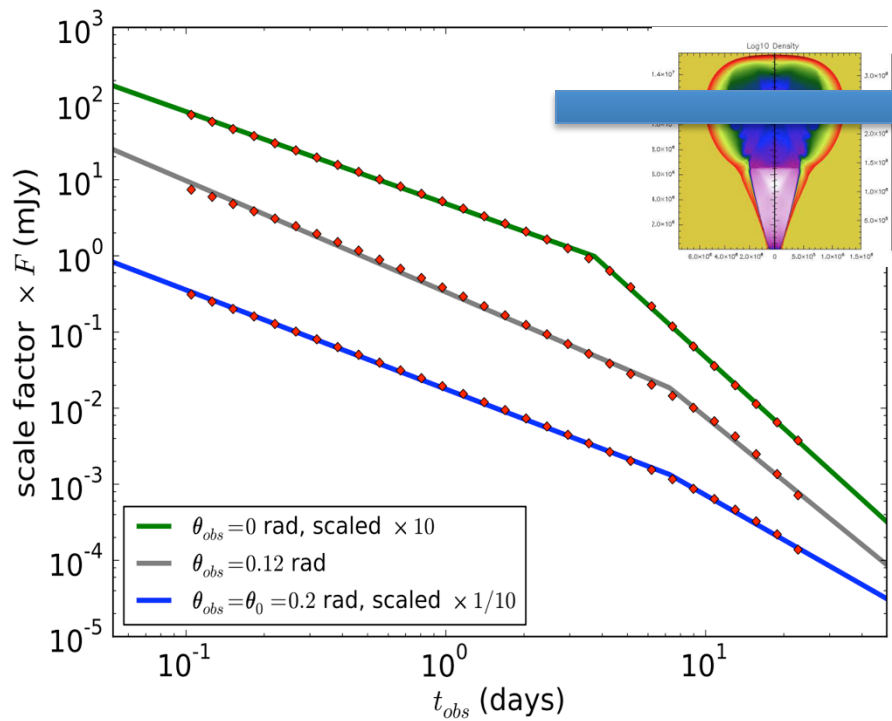
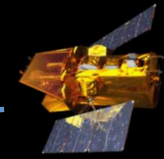
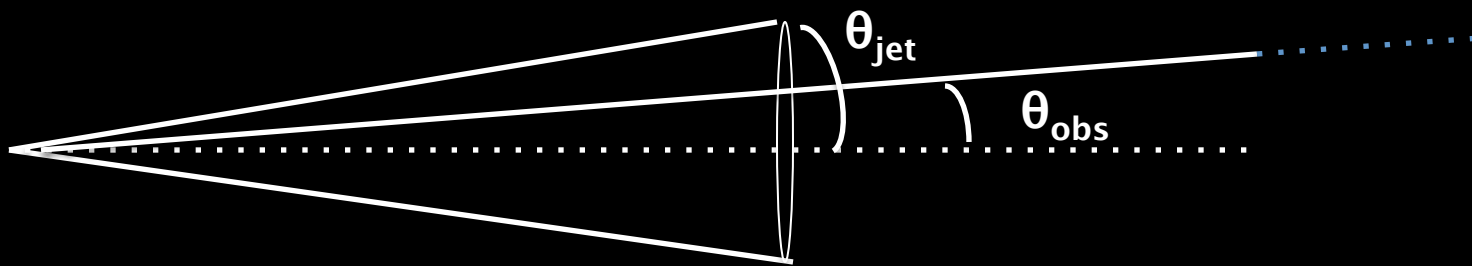
Large Viewing Angle Jet ? (but not directly off-axis jet)



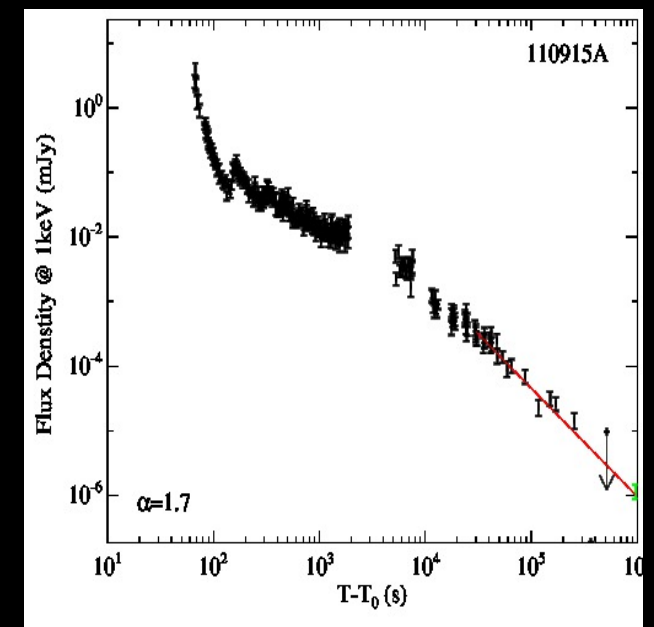
- More “realistic”
- Jet-breaks can be smeared out with large angles

van Eerten & MacFadyen 2012

Large Viewing Angle Jet ? (but not directly off-axis jet)



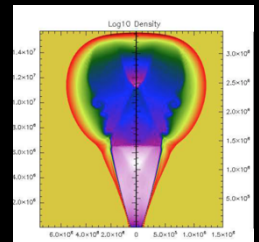
Fit Numerical simulations to Observations



Fit

- Thanks to the scaling relations for the full blast wave evolution (van Eerten & MacFadyen, 2011, 2012), we do not need to re-run the numerical simulations for every parameter configurations
- 7 free parameters

$$\theta_{\text{jet}}, \theta_{\text{obs}}, E_{\text{jet}}, p, n, \varepsilon_e, \varepsilon_B$$

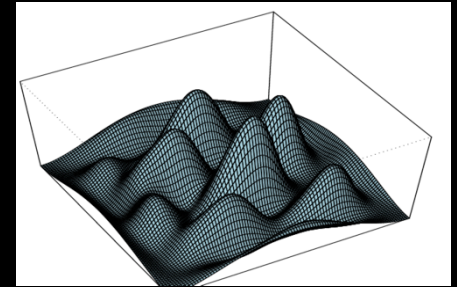


$\theta_{\text{jet}}, \theta_{\text{obs}}, E_{\text{jet}}, p, n, \epsilon_e, \epsilon_B$ + Numerical table

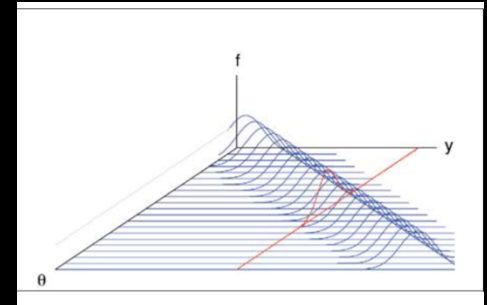


flux @ X-ray

- Degeneracy between parameters
(e.g, n and E_{jet})



- Non-Gaussian p-distribution in parameter space



- Insensitive parameters



Not suited to χ^2 fitting techniques



MCMC fit

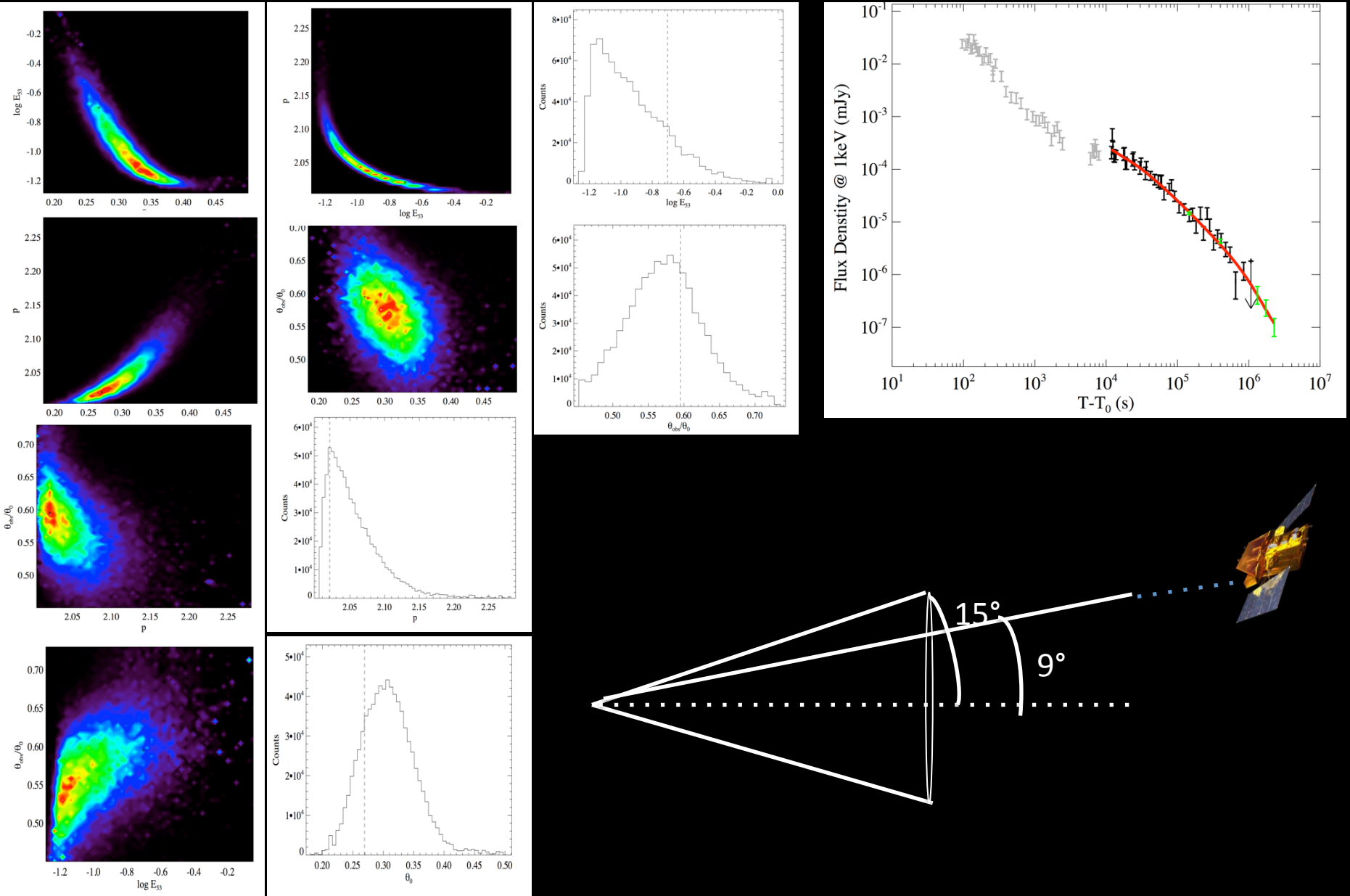
Our Codes

- An observation data handler
(for both Swift and Chandra)
Zhang, B.-B. et al 2007, 2008, 2009
- A numerical-simulation based “TABLE”
van Eerten et al 2010,2011,2012
- A flux calculator based on the scaling relations
van Eerten and MacFadyen 2012
- An improved fast MCMC sampler
multi-walker affine-invariant ensemble sampler;
Foreman-Mackey et al. 2013

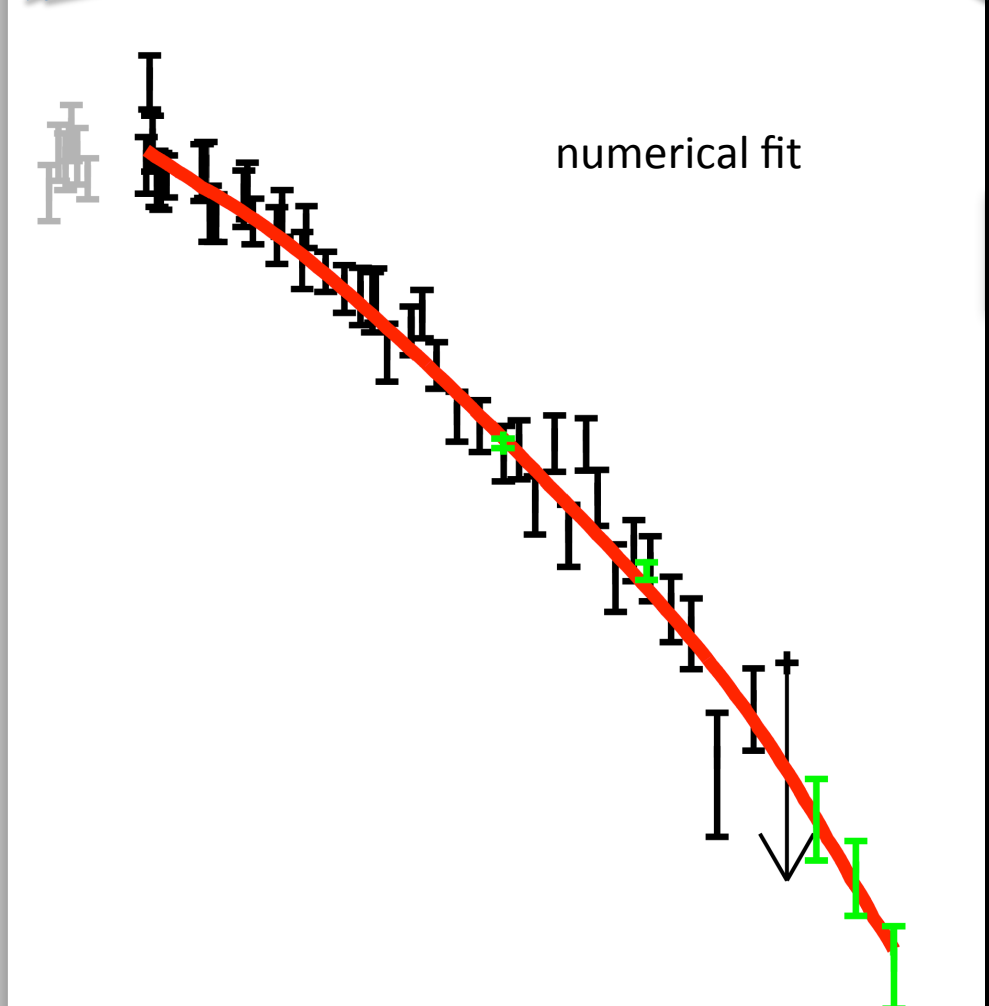
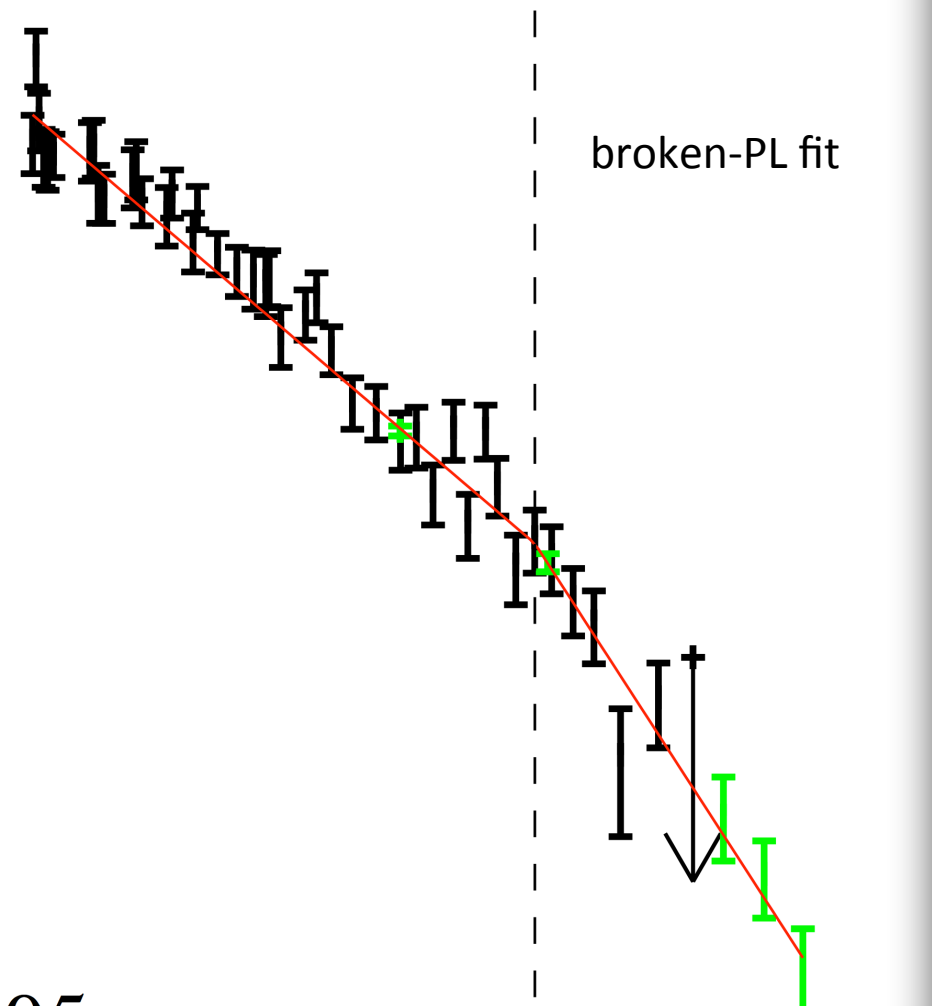
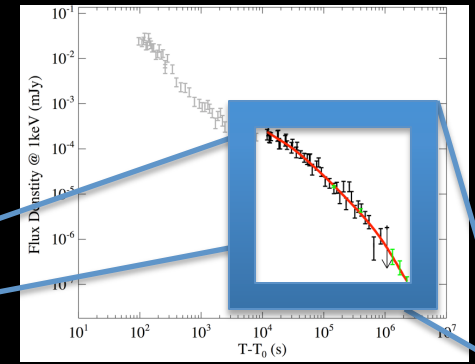
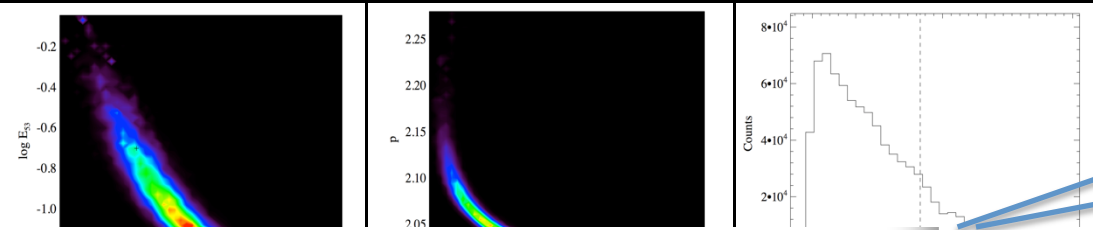


explain the data directly and more physically with numerical simulation

One Example



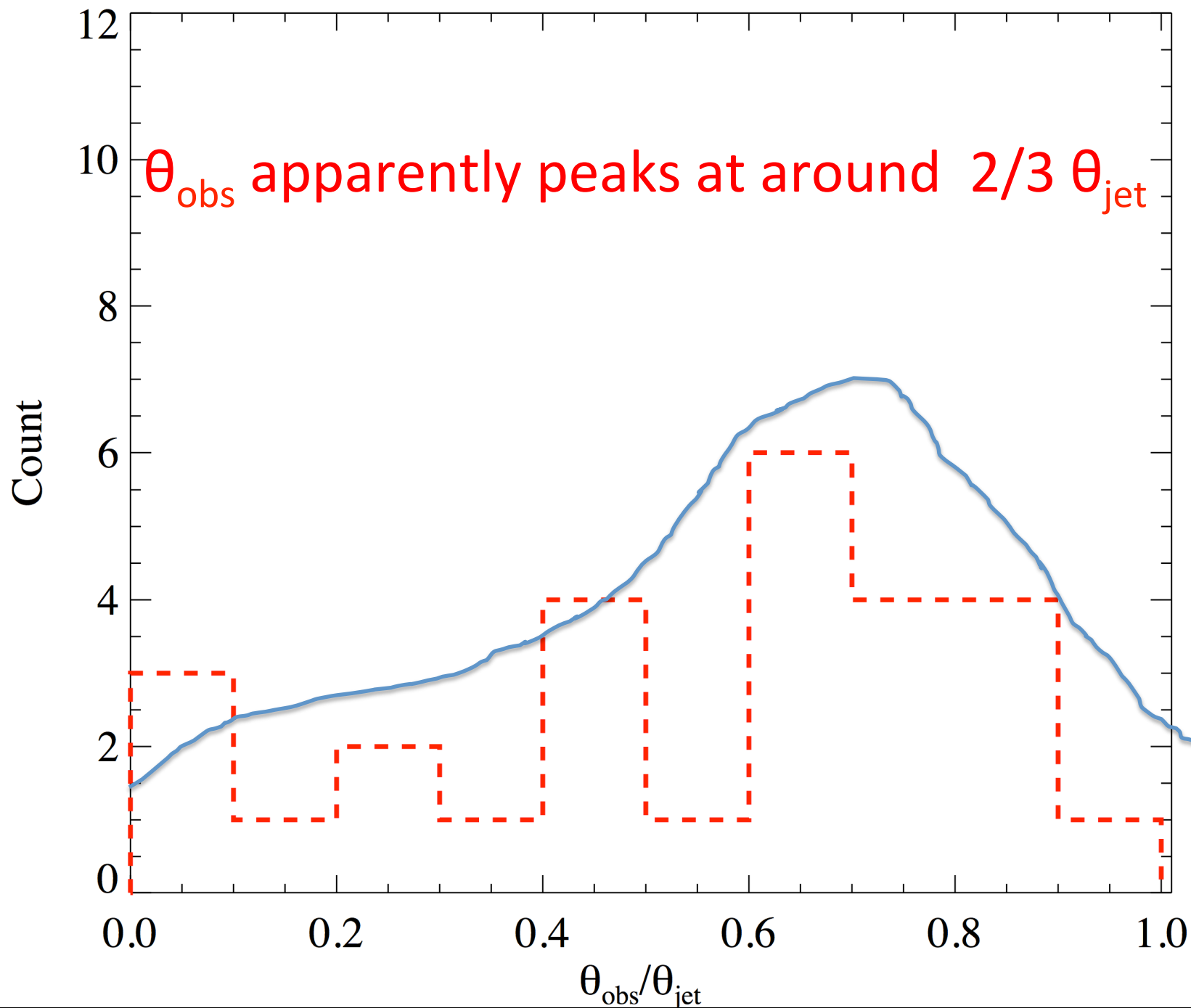
One Example



GRB	on-axis				off-axis				
	θ_{jet} rad	p	log E ₅₃ erg	χ^2/dof	θ_{jet} rad	$\frac{\theta_{obs}}{\theta_{jet}}$ rad	p	log E ₅₃ erg	χ^2/dof
051221	0.40 ^{+0.10} _{-0.03}	2.24 ^{+0.10} _{-0.07}	-1.21 ^{+0.12} _{-0.06}	46.7/43	0.27 ^{+0.11} _{-0.06}	0.60 ^{+0.13} _{-0.13}	2.02 ^{+0.11} _{-0.02}	-0.70 ^{+0.65} _{-0.51}	42.3/42
060729	0.39 ^{+0.06} _{-0.05}	2.46 ^{+0.03} _{-0.03}	0.83 ^{+0.04} _{-0.04}	520.9/43	0.40 ^{+0.08} _{-0.07}	0.97 ^{+0.03} _{-0.07}	2.46 ^{+0.09} _{-0.09}	0.83 ^{+0.18} _{-0.22}	520.7/43
061121	0.33 ^{+0.04} _{-0.09}	2.63 ^{+0.03} _{-0.05}	0.80 ^{+0.03} _{-0.04}	157.4/13	0.21 ^{+0.05} _{-0.03}	0.67 ^{+0.07} _{-0.07}	2.41 ^{+0.07} _{-0.06}	0.65 ^{+0.05} _{-0.04}	121.0/13
070125	0.05 ^{+0.02} _{-0.00}	2.04 ^{+0.10} _{-0.03}	1.16 ^{+0.31} _{-0.36}	175.4/21	0.05 ^{+0.02} _{-0.00}	0.20 ^{+0.60} _{-0.00}	2.04 ^{+0.16} _{-0.04}	1.15 ^{+0.34} _{-0.52}	185.3/20
071020	0.13 ^{+0.00} _{-0.08}	2.03 ^{+0.27} _{-0.02}	0.51 ^{+1.44} _{-0.38}	23.8/2	0.09 ^{+0.03} _{-0.04}	0.79 ^{+0.01} _{-0.78}	2.19 ^{+0.01} _{-0.19}	0.59 ^{+1.11} _{-0.35}	20.4/1
080207	0.33 ^{+0.02} _{-0.15}	2.92 ^{+0.11} _{-0.11}	0.61 ^{+0.09} _{-0.10}	27.9/33	0.31 ^{+0.04} _{-0.19}	0.88 ^{+0.02} _{-0.88}	2.70 ^{+0.35} _{-0.16}	0.47 ^{+0.23} _{-0.12}	26.9/32
080319B	0.27 ^{+0.08} _{-0.03}	2.33 ^{+0.30} _{-0.26}	0.15 ^{+0.49} _{-0.21}	134.9/49	0.32 ^{+0.03} _{-0.17}	0.35 ^{+0.64} _{-0.35}	2.33 ^{+0.23} _{-0.27}	0.16 ^{+0.37} _{-0.21}	96.1/48
081007	0.50 ^{+0.00} _{-0.10}	2.25 ^{+0.21} _{-0.17}	-0.87 ^{+0.32} _{-0.14}	32.8/19	0.49 ^{+0.01} _{-0.18}	0.86 ^{+0.14} _{-0.20}	2.05 ^{+0.26} _{-0.04}	-0.65 ^{+0.65} _{-0.24}	22.7/18
090102	0.43 ^{+0.07} _{-0.25}	2.58 ^{+0.05} _{-0.04}	0.48 ^{+0.04} _{-0.04}	108.6/91	0.32 ^{+0.18} _{-0.18}	0.79 ^{+0.10} _{-0.28}	2.45 ^{+0.08} _{-0.10}	0.40 ^{+0.06} _{-0.06}	95.6/90
090113	0.44 ^{+0.06} _{-0.20}	2.43 ^{+0.15} _{-0.14}	-0.31 ^{+0.18} _{-0.16}	14.4/8	0.33 ^{+0.17} _{-0.17}	0.12 ^{+0.87} _{-0.12}	2.05 ^{+0.27} _{-0.05}	-0.51 ^{+1.02} _{-0.21}	0.8/1
090417B	0.50 ^{+0.00} _{-0.09}	2.56 ^{+0.04} _{-0.04}	-0.34 ^{+0.04} _{-0.04}	123.8/11	0.47 ^{+0.03} _{-0.22}	0.88 ^{+0.12} _{-0.79}	2.37 ^{+0.19} _{-0.07}	-0.46 ^{+0.36} _{-0.05}	139.4/11
090423	0.12 ^{+0.09} _{-0.05}	2.42 ^{+0.17} _{-0.13}	0.63 ^{+0.07} _{-0.05}	31.0/42	0.08 ^{+0.42} _{-0.03}	0.68 ^{+0.24} _{-0.10}	2.19 ^{+0.37} _{-0.08}	0.68 ^{+0.24} _{-0.10}	39.2/41
091020	0.17 ^{+0.04} _{-0.02}	2.36 ^{+0.05} _{-0.05}	0.18 ^{+0.03} _{-0.03}	185.0/13	0.16 ^{+0.04} _{-0.04}	0.65 ^{+0.07} _{-0.13}	2.24 ^{+0.08} _{-0.10}	0.15 ^{+0.04} _{-0.02}	176.8/13
091127	0.13 ^{+0.03} _{-0.01}	2.13 ^{+0.09} _{-0.03}	0.14 ^{+0.05} _{-0.06}	724.7/37	0.50 ^{+0.00} _{-0.08}	0.82 ^{+0.12} _{-0.07}	2.40 ^{+0.16} _{-0.11}	0.20 ^{+0.35} _{-0.22}	82.0/56
100413A	0.17 ^{+0.33} _{-0.04}	2.37 ^{+0.36} _{-0.33}	-0.30 ^{+0.43} _{-0.21}	32.7/8	0.14 ^{+0.36} _{-0.06}	0.47 ^{+0.53} _{-0.47}	2.08 ^{+0.60} _{-0.06}	-0.32 ^{+0.52} _{-0.18}	34.5/7
100615A	0.16 ^{+0.01} _{-0.03}	2.32 ^{+0.14} _{-0.28}	0.32 ^{+0.23} _{-0.12}	128.5/26	0.14 ^{+0.36} _{-0.05}	0.46 ^{+0.52} _{-0.46}	2.09 ^{+0.35} _{-0.06}	0.34 ^{+0.35} _{-0.13}	107.3/25
100816A	0.50 ^{+0.00} _{-0.14}	2.04 ^{+0.02} _{-0.03}	-0.88 ^{+0.80} _{-0.12}	37.8/22	0.50 ^{+0.00} _{-0.15}	0.03 ^{+0.49} _{-0.03}	2.04 ^{+0.02} _{-0.04}	-0.89 ^{+0.96} _{-0.11}	38.1/21
101219B	0.50 ^{+0.00} _{-0.13}	2.00 ^{+0.00} _{-0.00}	0.62 ^{+0.06} _{-0.70}	43.7/17	0.50 ^{+0.00} _{-0.12}	0.01 ^{+0.59} _{-0.01}	2.00 ^{+0.00} _{-0.00}	0.62 ^{+0.06} _{-0.70}	43.8/16
110402A	0.20 ^{+0.19} _{-0.13}	2.69 ^{+0.39} _{-0.34}	-0.76 ^{+0.35} _{-0.24}	6.0/6	0.16 ^{+0.34} _{-0.11}	0.61 ^{+0.39} _{-0.61}	2.53 ^{+0.54} _{-0.43}	-0.90 ^{+0.65} _{-0.10}	6.9/5
110422A	0.07 ^{+0.02} _{-0.00}	2.23 ^{+0.03} _{-0.03}	0.49 ^{+0.02} _{-0.02}	443.2/25	0.06 ^{+0.01} _{-0.02}	0.65 ^{+0.05} _{-0.06}	2.09 ^{+0.03} _{-0.05}	0.74 ^{+0.25} _{-0.09}	416.7/25
110503A	0.14 ^{+0.01} _{-0.01}	2.33 ^{+0.06} _{-0.06}	0.40 ^{+0.05} _{-0.04}	181.5/12	0.18 ^{+0.11} _{-0.09}	0.67 ^{+0.11} _{-0.22}	2.25 ^{+0.09} _{-0.20}	0.37 ^{+0.26} _{-0.03}	154.6/12
110709B	0.06 ^{+0.01} _{-0.00}	2.00 ^{+0.00} _{-0.00}	2.76 ^{+0.04} _{-0.25}	634.9/33	0.06 ^{+0.00} _{-0.01}	0.49 ^{+0.06} _{-0.08}	2.00 ^{+0.00} _{-0.00}	2.79 ^{+0.01} _{-0.23}	656.8/32
110731A	0.38 ^{+0.12} _{-0.07}	2.25 ^{+0.05} _{-0.04}	0.48 ^{+0.03} _{-0.03}	61.3/45	0.43 ^{+0.07} _{-0.13}	0.28 ^{+0.32} _{-0.28}	2.26 ^{+0.05} _{-0.05}	0.49 ^{+0.03} _{-0.03}	59.1/44
110915A	0.07 ^{+0.03} _{-0.01}	2.01 ^{+0.23} _{-0.01}	0.64 ^{+0.54} _{-0.84}	127.8/49	0.06 ^{+0.11} _{-0.02}	0.43 ^{+0.57} _{-0.43}	2.00 ^{+0.44} _{-0.00}	1.24 ^{+0.19} _{-1.45}	143.0/48
111008A	0.10 ^{+0.02} _{-0.03}	2.11 ^{+0.06} _{-0.08}	1.13 ^{+0.31} _{-0.08}	175.0/11	0.09 ^{+0.03} _{-0.03}	0.71 ^{+0.09} _{-0.11}	2.08 ^{+0.09} _{-0.07}	1.22 ^{+0.64} _{-0.16}	187.9/11
120804A	0.50 ^{+0.00} _{-0.17}	2.03 ^{+0.06} _{-0.03}	-0.36 ^{+0.86} _{-0.30}	29.5/16	0.50 ^{+0.00} _{-0.18}	0.02 ^{+0.62} _{-0.02}	2.03 ^{+0.07} _{-0.03}	-0.35 ^{+0.85} _{-0.34}	29.5/15
121027A	0.29 ^{+0.04} _{-0.09}	2.73 ^{+0.09} _{-0.14}	1.33 ^{+0.14} _{-0.22}	51.9/46	0.20 ^{+0.30} _{-0.09}	0.71 ^{+0.29} _{-0.71}	2.38 ^{+0.45} _{-0.20}	0.94 ^{+0.59} _{-0.24}	62.5/45

GRB	on-axis				off-axis				
	θ_{jet}	p	log E ₅₃	χ^2/dof	θ_{jet}	$\frac{\theta_{obs}}{\theta_{jet}}$	p	log E ₅₃	χ^2/dof
	rad		erg		rad	rad		erg	
051221	0.40 ^{+0.10} _{-0.03}	2.24 ^{+0.10} _{-0.07}	-1.21 ^{+0.12} _{-0.06}	46.7/43	0.27 ^{+0.11} _{-0.06}	0.60 ^{+0.13} _{-0.13}	2.02 ^{+0.11} _{-0.02}	-0.70 ^{+0.65} _{-0.51}	42.3/42
060729	0.39 ^{+0.06} _{-0.05}	2.46 ^{+0.03} _{-0.03}	0.83 ^{+0.04} _{-0.04}	520.9/434	0.40 ^{+0.08} _{-0.07}	0.97 ^{+0.03} _{-0.07}	2.46 ^{+0.09} _{-0.09}	0.83 ^{+0.18} _{-0.22}	520.7/433
061121	0.33 ^{+0.04} _{-0.09}	2.63 ^{+0.03} _{-0.05}	0.80 ^{+0.03} _{-0.04}	157.4/137	0.21 ^{+0.05} _{-0.03}	0.67 ^{+0.07} _{-0.07}	2.41 ^{+0.07} _{-0.06}	0.65 ^{+0.05} _{-0.04}	121.0/136
070125	0.05 ^{+0.02} _{-0.00}	2.04 ^{+0.10} _{-0.03}	1.16 ^{+0.31} _{-0.36}	175.4/21	0.05 ^{+0.02} _{-0.00}	0.20 ^{+0.60} _{-0.00}	2.04 ^{+0.16} _{-0.04}	1.15 ^{+0.34} _{-0.52}	185.3/20
071020	0.13 ^{+0.00} _{-0.08}	2.03 ^{+0.27} _{-0.02}	0.51 ^{+1.44} _{-0.38}	23.8/2	0.09 ^{+0.03} _{-0.04}	0.79 ^{+0.01} _{-0.78}	2.19 ^{+0.01} _{-0.19}	0.59 ^{+1.11} _{-0.35}	20.4/1
080207	0.33 ^{+0.02} _{-0.15}	2.92 ^{+0.11} _{-0.11}	0.61 ^{+0.09} _{-0.10}	27.9/33	0.31 ^{+0.04} _{-0.19}	0.88 ^{+0.02} _{-0.88}	2.70 ^{+0.35} _{-0.16}	0.47 ^{+0.23} _{-0.12}	26.9/32
080319B	0.27 ^{+0.08} _{-0.03}	2.33 ^{+0.30} _{-0.26}	0.15 ^{+0.49} _{-0.21}	134.9/49	0.32 ^{+0.03} _{-0.17}	0.35 ^{+0.64} _{-0.35}	2.33 ^{+0.23} _{-0.27}	0.16 ^{+0.37} _{-0.21}	96.1/48
081007	0.50 ^{+0.00} _{-0.10}	2.25 ^{+0.21} _{-0.17}	-0.87 ^{+0.32} _{-0.14}	32.8/19	0.49 ^{+0.01} _{-0.18}	0.86 ^{+0.14} _{-0.20}	2.05 ^{+0.26} _{-0.04}	-0.65 ^{+0.65} _{-0.24}	22.7/18
090102	0.43 ^{+0.07} _{-0.25}	2.58 ^{+0.05} _{-0.04}	0.48 ^{+0.04} _{-0.04}	108.6/91	0.32 ^{+0.18} _{-0.18}	0.79 ^{+0.10} _{-0.28}	2.45 ^{+0.08} _{-0.10}	0.40 ^{+0.06} _{-0.06}	95.6/90
091118	0.44 ^{+0.06} _{-0.20}	2.43 ^{+0.15} _{-0.11}	-0.31 ^{+0.18} _{-0.16}	14.4/8	0.33 ^{+0.17} _{-0.17}	0.12 ^{+0.87} _{-0.12}	2.05 ^{+0.27} _{-0.05}	-0.51 ^{+1.02} _{-0.21}	0.8/1
090417B	0.50 ^{+0.00} _{-0.09}	2.56 ^{+0.04} _{-0.04}	-0.34 ^{+0.04} _{-0.04}	123.8/119	0.47 ^{+0.03} _{-0.22}	0.88 ^{+0.02} _{-0.79}	2.37 ^{+0.09} _{-0.77}	-0.46 ^{+0.16} _{-0.15}	130.4/118
090423	0.12 ^{+0.09} _{-0.05}	2.42 ^{+0.17} _{-0.13}	0.63 ^{+0.07} _{-0.05}	31.0/42	0.08 ^{+0.42} _{-0.03}	0.68 ^{+0.24} _{-0.10}	2.19 ^{+0.37} _{-0.08}	0.68 ^{+0.10} _{-0.10}	39.2/41
091020	0.17 ^{+0.04} _{-0.02}	2.36 ^{+0.05} _{-0.05}	0.18 ^{+0.03} _{-0.03}	185.0/131	0.16 ^{+0.04} _{-0.04}	0.65 ^{+0.07} _{-0.13}	2.24 ^{+0.08} _{-0.10}	0.15 ^{+0.04} _{-0.02}	176.8/130
091127	0.13 ^{+0.03} _{-0.01}	2.13 ^{+0.09} _{-0.03}	0.14 ^{+0.05} _{-0.06}	724.7/370	0.50 ^{+0.00} _{-0.08}	0.82 ^{+0.12} _{-0.07}	2.40 ^{+0.16} _{-0.11}	0.20 ^{+0.35} _{-0.22}	82.0/56
100413A	0.17 ^{+0.33} _{-0.04}	2.37 ^{+0.36} _{-0.33}	-0.30 ^{+0.43} _{-0.21}	32.7/8	0.14 ^{+0.36} _{-0.06}	0.47 ^{+0.53} _{-0.47}	2.08 ^{+0.60} _{-0.06}	-0.32 ^{+0.52} _{-0.18}	34.5/7
100615A	0.16 ^{+0.01} _{-0.03}	2.32 ^{+0.14} _{-0.28}	0.32 ^{+0.23} _{-0.12}	128.5/26	0.14 ^{+0.36} _{-0.05}	0.46 ^{+0.52} _{-0.46}	2.09 ^{+0.35} _{-0.06}	0.34 ^{+0.35} _{-0.13}	107.3/25
100816A	0.50 ^{+0.00} _{-0.14}	2.04 ^{+0.02} _{-0.03}	-0.88 ^{+0.80} _{-0.12}	37.8/22	0.50 ^{+0.00} _{-0.15}	0.03 ^{+0.49} _{-0.03}	2.04 ^{+0.02} _{-0.04}	-0.89 ^{+0.96} _{-0.11}	38.1/21
101219B	0.50 ^{+0.00} _{-0.13}	2.00 ^{+0.00} _{-0.00}	0.62 ^{+0.06} _{-0.70}	43.7/17	0.50 ^{+0.00} _{-0.12}	0.01 ^{+0.59} _{-0.01}	2.00 ^{+0.00} _{-0.00}	0.62 ^{+0.06} _{-0.70}	43.8/16
110402A	0.20 ^{+0.19} _{-0.13}	2.69 ^{+0.39} _{-0.34}	-0.76 ^{+0.35} _{-0.24}	6.0/6	0.16 ^{+0.34} _{-0.11}	0.61 ^{+0.39} _{-0.61}	2.53 ^{+0.54} _{-0.43}	-0.90 ^{+0.65} _{-0.10}	6.9/5
110422A	0.07 ^{+0.02} _{-0.00}	2.23 ^{+0.03} _{-0.03}	0.49 ^{+0.02} _{-0.02}	443.2/259	0.06 ^{+0.01} _{-0.02}	0.65 ^{+0.05} _{-0.06}	2.09 ^{+0.03} _{-0.05}	0.74 ^{+0.25} _{-0.09}	416.7/258
110503A	0.14 ^{+0.01} _{-0.01}	2.33 ^{+0.06} _{-0.06}	0.40 ^{+0.05} _{-0.04}	181.5/122	0.18 ^{+0.11} _{-0.09}	0.67 ^{+0.11} _{-0.22}	2.25 ^{+0.09} _{-0.20}	0.37 ^{+0.26} _{-0.03}	154.6/121
110709B	0.06 ^{+0.01} _{-0.00}	2.00 ^{+0.00} _{-0.00}	2.76 ^{+0.04} _{-0.25}	634.9/330	0.06 ^{+0.00} _{-0.01}	0.49 ^{+0.06} _{-0.08}	2.00 ^{+0.00} _{-0.00}	2.79 ^{+0.01} _{-0.23}	656.8/329
110731A	0.38 ^{+0.12} _{-0.07}	2.25 ^{+0.05} _{-0.04}	0.48 ^{+0.03} _{-0.03}	61.3/45	0.43 ^{+0.07} _{-0.13}	0.28 ^{+0.32} _{-0.28}	2.26 ^{+0.05} _{-0.05}	0.49 ^{+0.03} _{-0.03}	59.1/44
110915A	0.07 ^{+0.03} _{-0.01}	2.01 ^{+0.23} _{-0.01}	0.64 ^{+0.54} _{-0.84}	127.8/49	0.06 ^{+0.11} _{-0.02}	0.43 ^{+0.57} _{-0.43}	2.00 ^{+0.44} _{-0.00}	1.24 ^{+0.19} _{-1.45}	143.0/48
111008A	0.10 ^{+0.02} _{-0.03}	2.11 ^{+0.06} _{-0.08}	1.13 ^{+0.31} _{-0.08}	175.0/113	0.09 ^{+0.03} _{-0.03}	0.71 ^{+0.09} _{-0.11}	2.08 ^{+0.09} _{-0.07}	1.22 ^{+0.64} _{-0.16}	187.9/112
120804A	0.50 ^{+0.00} _{-0.17}	2.03 ^{+0.06} _{-0.03}	-0.36 ^{+0.86} _{-0.30}	29.5/16	0.50 ^{+0.00} _{-0.18}	0.02 ^{+0.62} _{-0.02}	2.03 ^{+0.07} _{-0.03}	-0.35 ^{+0.85} _{-0.34}	29.5/15
121027A	0.29 ^{+0.04} _{-0.09}	2.73 ^{+0.09} _{-0.14}	1.33 ^{+0.14} _{-0.22}	51.9/46	0.20 ^{+0.30} _{-0.09}	0.71 ^{+0.29} _{-0.71}	2.38 ^{+0.45} _{-0.20}	0.94 ^{+0.59} _{-0.24}	62.5/45

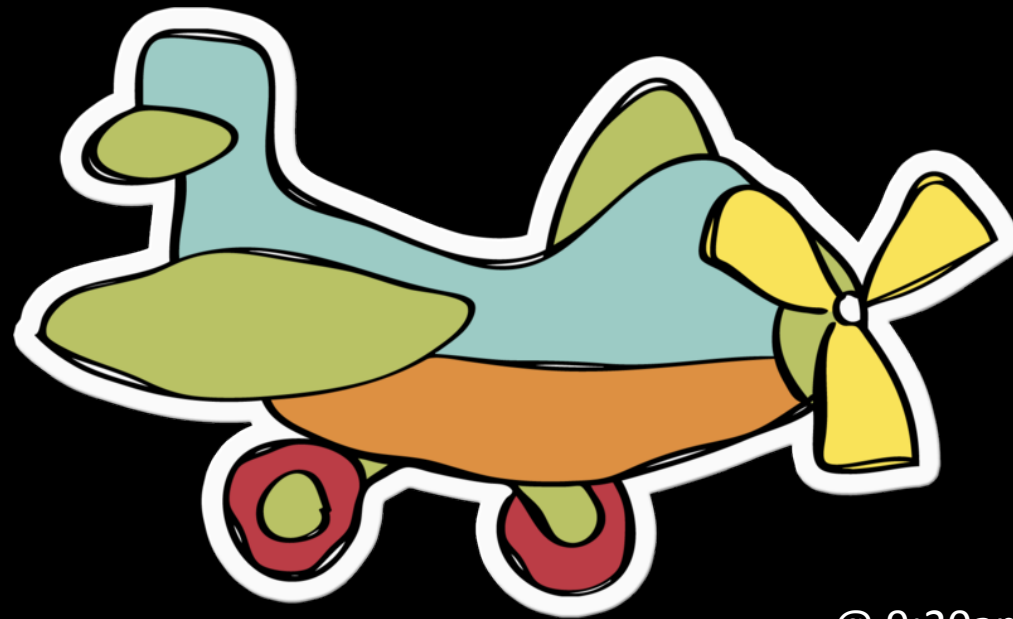
Data naturally favor off-axis jets



Summary

- More jet-breaks (50% vs 12%) in Chandra GRBs
- Late breaks (10^6 vs 10^5 s)
- The hidden jet-break problem can be naturally and physically explained by off-axis jets by fitting numerical results to observational data
- We are more likely not staring at the jet direction, but about 2/3 off-axis.

Thanks !



@ 9:20am